# Interferometer-Based Amplitude and Phase Calibration for Beam-Forming Systems

Hsien-Tung Huang, Ruey-Bing Hwang, *Senior Member, IEEE*

***Abstract*—As far as a beam-forming system is concerned, the dynamic adjustment of the phase angle on each radio frequency (RF) signal connected to antenna element should be taken into account. In this paper, we report the phase calibration scheme for a beam-forming architecture based on phase-adjustable local oscillator (LO) made of I/Q modulator. One degree phase shifting resolution was obtained by using the 14 bit analog-to-digital converter. The on-board calibration circuit by detecting the combined power level of the two LO signals under calibration is designed, implemented and measured.**

***Index Terms*—phase-shifting local oscillator, phase calibration techniques, beam-forming system, array antennas.**

## I. Introduction

BEAM steering technology has long been a hot research topic in microwave and millimeter wave radar system [1], [2]. The basic architecture and theory for passive and active phased arrays have been reported [3], [4]. The array phenomena was extensively and intensively studied [5]. In addition to radar system, a fully integrated UWB beam-former for imaging applications featuring controllable true time delay and power gain was researched [6]. The beam-forming mechanism usually is based on dynamically changing the weighting factor including the phase and amplitude of the radio frequency (RF) signal fed to each array antenna. Moreover, the beam-forming based on the adaptive signal processing has played an important role in modern sensor system like radar and sonar [7]. Recently, the fifth generation (5G) emerging technology for wireless communication attracts considerable attention due to its high data-rate transmission, beam-tracking, and beam-forming capabilities [8].

Specifically, the beam-forming and beam-tracking technologies can significantly enhance the system signal-to-noise ratio and also extend the transmission range.

In a transmitter architecture, a vector modulator is employed to convert the baseband I (in-phase) and Q (quadrature) signals into RF (homodyne) or Intermediate frequency (heterodyne) one via a local oscillator, with the mathematical expression given below.

$$f_{RF}(t) = i(t)\cos\omega_0 t + q(t)\sin\omega_0 t \tag{1}$$

The authors are with the Department of Electrical Engineering, National Chiao-Tung University, 300 Hsinchu, Taiwan.(corresponding author: Professor Ruey-Bing Hwang; e-mail: raybeam@mail.nctu.edu.tw). Ruey-Bing Hwang conceived the idea of calibration mechanism using interferometry; Hsien-Tung Huang completed the circuit design and measurement consisting of the phased local oscillators and interferometers. The authors thank Mr. C.-W. Chang for his help in conducting the antennas radiation pattern measurement.

where $f_{RF}(t)$, $i(t)$ and $q(t)$ are the RF output, in-phase, and quadrature baseband signals, respectively. Parameter $\omega_0$ is the angular frequency of the local oscillator.

There are three ways to manipulate the phase angle at the RF output. The first one is to change the phase angle over the baseband I and Q signals (in the digital domain). This solution needs sophisticated computing power, and high-speed and high-resolution digital-to-analog conversion (DAC) technique; however, no dedicated phase shifting block is required. The second way is to alter the phase angle directly at the RF path by a phase shifter [9]. Unfortunately, the phase shifting is a nonlinear process in particular for the use of higher level modulation such as 64-QAM with varying envelop; a complicated calibration is usually needed. The third way is to vary the phase angle at the local oscillator. The first scheme is the so-called digital beam-forming; the second one is the commonly used analog beam-forming.

Here, we adopt the third strategy by changing the phase angle over the local oscillator. Such a phase-adjustable local oscillators scheme can be used in both transmitter- and receiver- beam-forming architectures, and has been reported in the literature. To mention a few, a 5.2 GHz CMOS I/Q modulator with integrated phase shifter was reported [10] to have a phase shifting resolution of $10^o$ by using a 6 bit DAC. For a sophisticated beam-forming scenario in a smart antenna or radar system, one needs a phase shifting resolution much less than $10^o$. A broadband phase shifter was fabricated by assembling the Langer coupler, I/Q modulator and multi-section Wilkinson power divider in a microwave printed circuit board. The four phase shifting angles including $0^o$, $90^o$, $180^o$, and $270^o$ were measured in a wide bandwidth [11]. Additionally, the phase-adjustable local oscillator can also be implemented by adding a narrow band phase shifter behind a stable local oscillator; the beam-steering characteristics in a frequency-modulation continuous-wave radar system has been experimentally verified [12].

In this research, we design a phase-adjustable LO array consisting of 4 on-shelf I/Q modulators for a beam-forming system. The in-phase and quadrature signals are given by a multiple channel analog card each output equipped with a 14-bit DAC. Notably, in our system scenarios, the phase angles of the array are provided by the LO signal only, in particular at a specific frequency. We do not need a wide-band I/Q modulator.

The system block is shown in Fig.1. A local oscillator signal generated by a synthesizer at 2.4 GHz is equally divided into 4 ways and fed in each I/Q modulator. We may adjust the output RF phase by manipulating the I/Q signals, as will become clear later on. The slits are on the ground plane

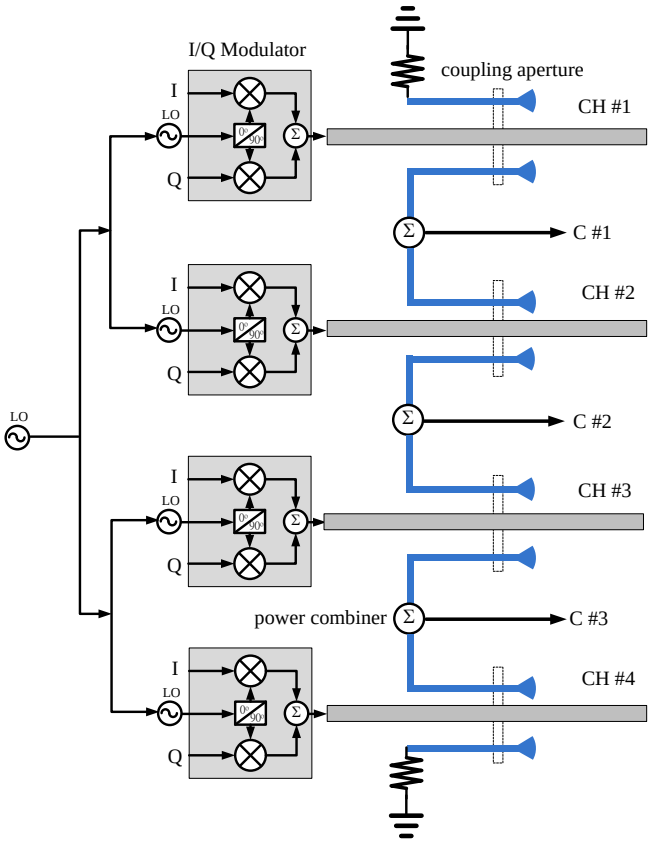


Fig. 1. System block of the 4-channel phase-adjustable local oscillators equipped with the on-board calibration circuit.

behind the micro-strip lines for aperture coupled function. Each Wilkinson power combiner on the other side (below the ground plane) combines the coupled signals from the two adjacent RF outputs. We then detect the variation of combined power level against the phase control of each I/Q modulator to calibrate the phase distribution of the system.

## II. I/Q MODULATOR-BASED PHASED LOCAL OSCILLATOR

Returning to equation (1), if the baseband I and Q signals are *dc* (time independent) voltage, such as $i$ and $q$, the output signal can be written as:

$$f_{RF}(t) = \sqrt{i^2 + q^2}\cos(\omega_0 t - \tan^{-1}\frac{q}{i}) \qquad (2)$$

Thus, we may change the phase angle of the output signal through the *dc* I and Q signals without altering the frequency of local oscillator. Here the RFICs vector modulator (*Hittite* HMC631) was employed to change the phase angle of the local oscillator by feeding the *dc* I and Q signals generated by a 14-bits DAC system. The local oscillator works at single frequency 2.4 GHz generated by a phase-locked loop (PLL) synthesizer.

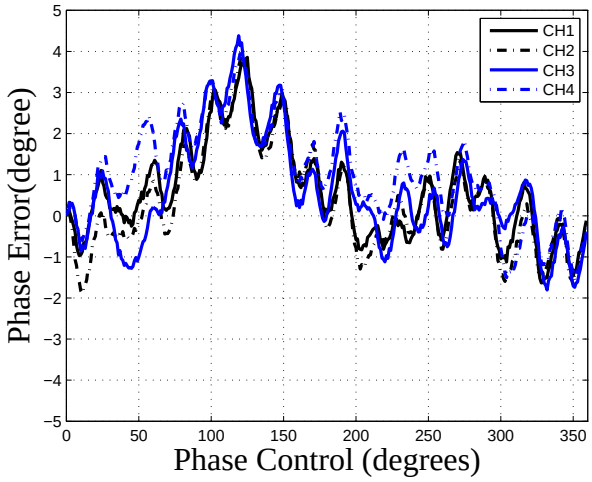


Fig. 2. Measurement of the phase error corresponding to each vector modulator.

## III. PHASE CALIBRATION CIRCUIT AND METHODOLOGY

In this section, we propose an efficient way for calibrating the two RF outputs with different phase angles and amplitudes. Here the two signals have, respectively, voltage $a_1 e^{j\phi_1}$ and $a_2 e^{j\phi_2}$, where the time harmonic $\exp(j\omega t)$ is suppressed due to phasor notation. The combined voltage (sum) of the two RF signals through an ideal power combiner is equal to:

$$v_o = a_1 e^{j\phi_1} + a_2 e^{j\phi_2} = a_1 e^{j\phi_1}(1 + \frac{a_2}{a_1} e^{j\Delta\phi}) \qquad (3)$$

Where $\Delta\phi$ is the phase angle deviation between the two RF signals. Notably, we assume that the two arms of the power combiner will not introduce any phase difference between them.

Figure 3 depicts the variation on the output combining voltage normalized to $a_1 + a_2$ against the phase angle at the second port, while the phase angle at the first port is assumed to be $100^o$. The three cases with different voltage ratio ($r = a_2/a_1$), shown in the legend, were calculated. Through scanning the phase angle at the second port, the maximum combining power was found to occur at $\phi_2 = 100^o$ accordingly. Furthermore, the output voltage gradually vanishes at the out-of-phase condition, this allows us to adjust the weighting to have the equal power.

To validate the aforementioned mechanism, we carry out a measurement with the experimental setup shown in Fig.4. The power incident to port 1 is divided into two paths transmitted trough a delay line plus an attenuator and the I/Q modulator, respectively. The attenuator employed here is to balance the conversion loss of the vector modulator. After combining the two signals via the other Wilkinson power combiner at port 2, we may measure the insertion loss through a vector network analyzer.

Figure 5 shows the insertion loss versus phase control over the vector modulator by dynamically changing the phase angle from $0^o$ to $360^o$ with one degree increment. Apparently, there are maximums and minimum respectively corresponding to the in-phase and out-of-phase responses present in the

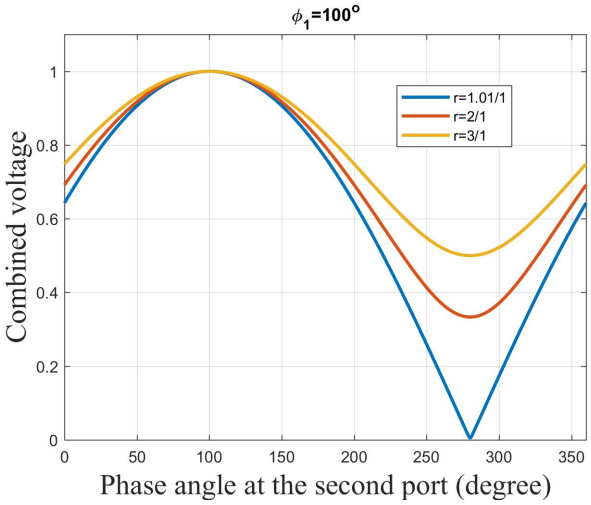


Fig. 3. Combined voltage amplitude at the ideal power combinator against the phase angle at the second port; the phase angle at the first port is assumed to be $100^o$.

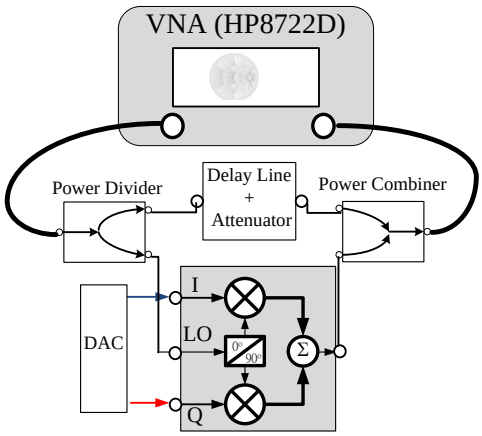


Fig. 4. Experimental setup for proving the power combining mechanism used in phase calibration.

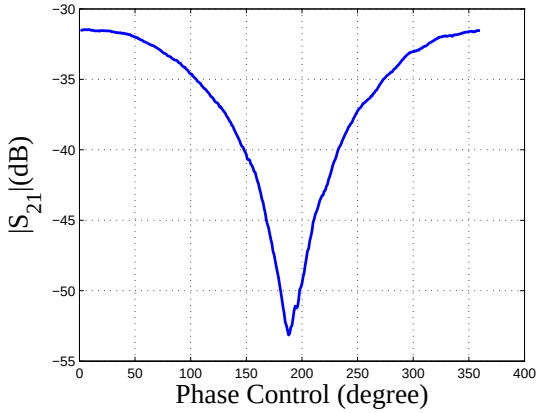


Fig. 5. Measurement of the combined power normalized to the incident power.

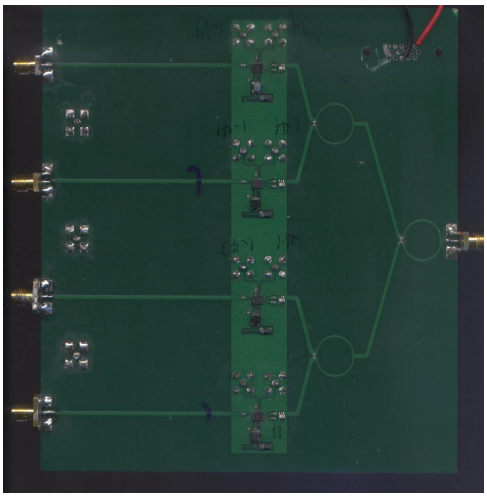

Fig. 6. Top layer of the pcb.

figure. Notably, the in-phase response is insensitive to the phase control; on the other hand, the out-of-phase exhibits an obvious lobe at $188^o$. It allows us to pinpoint the phase angle from the out-of-phase response rather than from the in-phase one. Therefore, the phase delay angle of the delay line plus attenuator should be 8 degree.

## IV. Implementation of the 4-channel phase-adjustable local oscillators

Figures 6 and 7 depict the photos of the printed circuit board of the 4-channel phase-adjustable local oscillators. Referring to Fig.1, the Wilkinson power combiners combine the two RF signals coupled from the outputs of the two adjacent vector modulators, respectively. In order not to affect the signal amplitude and phase, around -17 dB coupling coefficient is designed for the aperture coupled structure. Additionally, to maintain the symmetry of the structure, the two extra coupled lines are designed and terminated to a 50 Ω load.

Regarding the phase calibration process, we first fix the phase angle of the first channel. Secondly, we dynamically change the phase control of the second vector modulator from 0 to 360 degree. The minimum combined power like the figure shown in Fig.5 can pinpoint the out-of-phase angle of the second vector modulator; the in-phase angle can be determined accordingly. Moreover, we may take the phase angle of the second one as a reference and repeat the aforementioned procedure; the phase angle of the third one can be correctly decided. We may easily determine the phase angle on the fourth I/Q modulator in the same manner.

Since the phase angle of each vector modulator can also be independently measured using the vector network analyzer by terminating the other three output ports with 50Ω loads. After finishing the phase calibration procedure described previously, the histogram of the phase angle over each path is drawn from Fig.8 to 11, respectively. The maximum deviation of the average angles is around 1.186 degree.

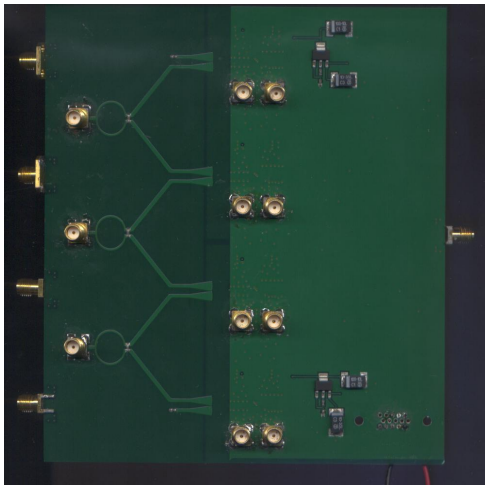

Fig. 7. Bottom layer of the pcb.

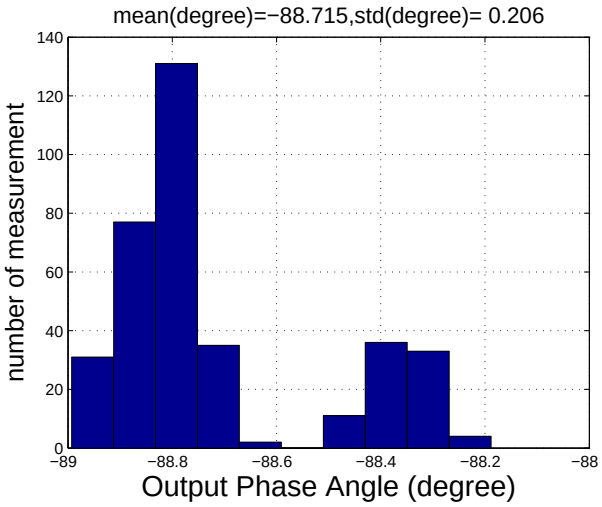


Fig. 8. Histogram of the phase angle measured from vector network analyzer of channel 1; mean and standard deviation are $-88.715^o$ and $0.206^o$, respectively.

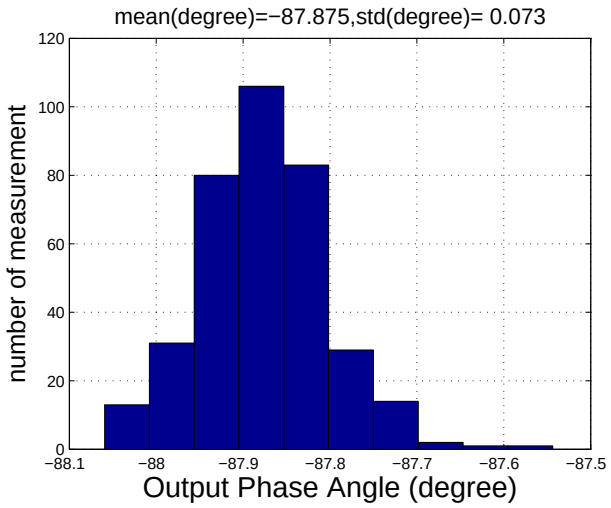


Fig. 9. Histogram of the phase angle measured from vector network analyzer of channel 2; mean and standard deviation are $-87.875^o$ and $0.073^o$, respectively.

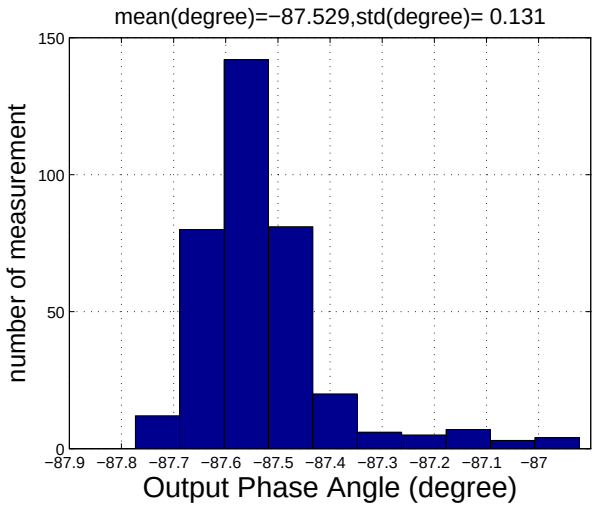


Fig. 10. Histogram of the phase angle measured from vector network analyzer of channel 3; mean and standard deviation are $-87.529^o$ and $0.131^o$, respectively.

## V. Measurement of Beam-Steering Characteristics

To demonstrate the accurate phase control capability, we directly connect the 4-way phase-adjustable LO outputs to a uniform linear array consisting of 4 printed Yagi antennas with the PCB layout shown in Fig. 12 and 13. As we know, an array antenna can adjust the phase of each element so that the propagation delays of the transmitted signals received by them are compensated for a particular direction. Consequently, for a uniform linear array with period $d$ (where $d$ is smaller than half-wavelength for eliminating the grating lobes), the relationship between the radiation main-beam angle ($\theta$) and progressive delay angle ($\Delta\psi$) between two adjacent elements are given below:

$$\Delta\psi + k_o d \sin\theta = 0 \tag{4}$$

where $k_o = 2\pi/\lambda$, and $\lambda$ is the wavelength in free-space.

Before demonstrating the array pattern, the radiation characteristics of each antenna element are measured and verified their consistency. Figure 14 shows the reflection coefficient of the four antennas. At 2.4 GHz, they all have the reflection coefficient below -15dB. Figure 15 depicts the radiation pattern on the $x$-$z$ plane. Obviously, their radiation patterns are consistent ranging from $-90^o$ to $+90^o$.

We then integrate the antennas and 4-way LO signals to verify their beam-forming capability. The four antennas are arranged as a one-dimensional uniform array with period 60 mm along the $z$-axis (the coordinate system is attached in Fig. 12). The period is around 0.48 wavelength at 2.4 GHz.The vertical polarization of the array antenna is of primary concern.

Figure 16 shows the radiation pattern for several progressive phase-delay angles depicted in the legend. It is obvious to see that the main-beam angle swings in accordance with the

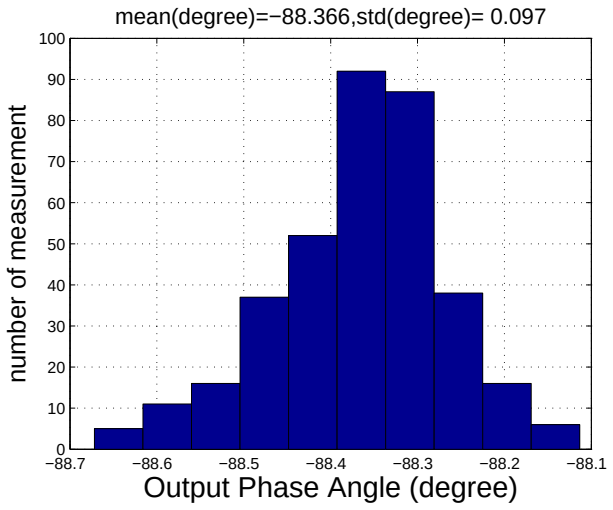


Fig. 11. Histogram of the phase angle measured from vector network analyzer of channel 4; mean and standard deviation are $-88.366^o$ and $0.097^o$, respectively.

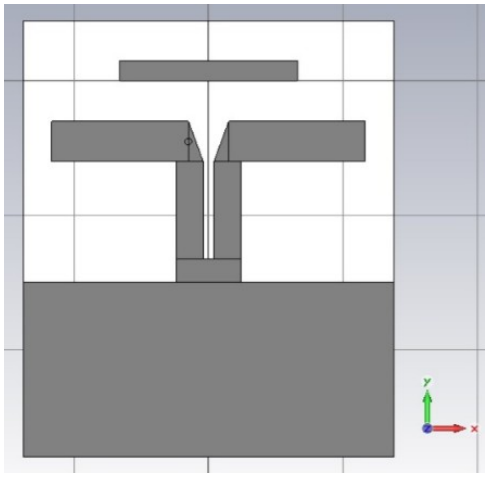

Fig. 12. PCB layout of the printed Yagi antenna employed in the beam-forming array system (top layer).

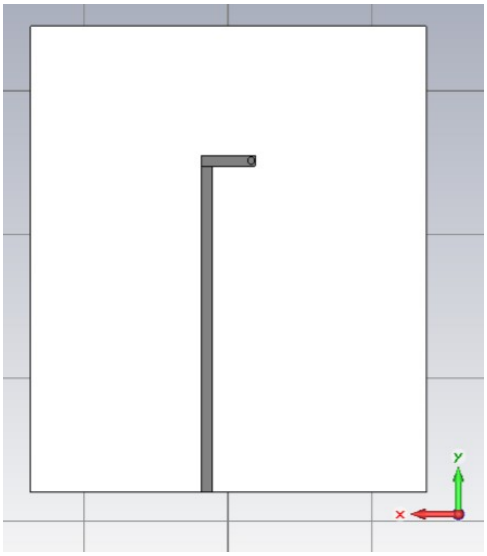

Fig. 13. PCB layout of the printed Yagi antenna employed in the beam-forming array system (bottom layer.)

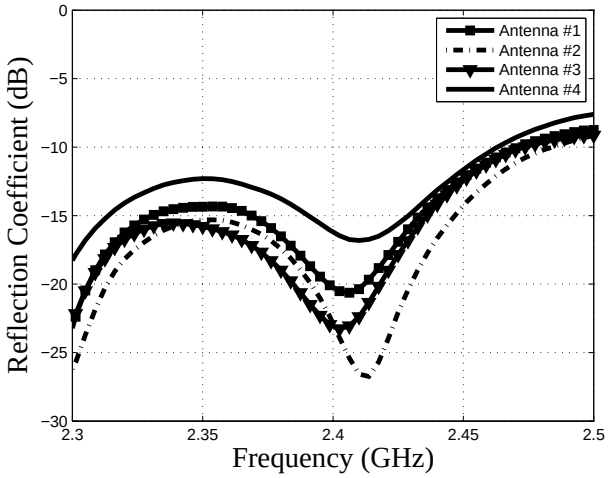


Fig. 14. Measured reflection coefficient of the 4 printed Yagi antennas.

change in $\Delta\psi$. The peak gain of the array antenna roughly approaches 10 dBi for every single beam-forming case. Due to the 4 printed Yagi antennas with slightly inconsistent peak gains, the array peak gain drops about 1 dBi compared with the theoretical calculation.

## VI. Conclusion

In this paper, a network for generating the 4-way phase-shifting local oscillator signals was designed, implemented and measured. Specifically, the phase calibration circuit is also designed together with the phase-shifting LO network. Through detecting the out-of-phase combining power between adjacent output LO signals, we may immediately monitor the LO phase angles. To demonstrate the capability of accurate phase control over the phase-shifting LO signals, we directly connect them to a printed Yagi antennas array and measure the radiation pattern while beam-forming. In comparison with the traditionally used RF phase shifter, such a beam-forming architecture using phase-shifting LO is an cost-effective technology and may be a potential candidate for serving as the smart antenna system applied in the next-generation wireless communications system.

## Acknowledgement

The authors would thank CST-Computer Simulation Technology and ROHDE&SCHWARZ Taiwan for their support in providing us the software and measurement facilities, respectively.

## References

[1] M. Skolnik, *Introduction to Radar Systems*, 2001: McGraw-Hill
[2] M. Skolnik, "Role of radar in microwaves," *Microwave Theory and Techniques, IEEE Transactions on*, vol.50, no.3, pp.625–632, Mar 2002

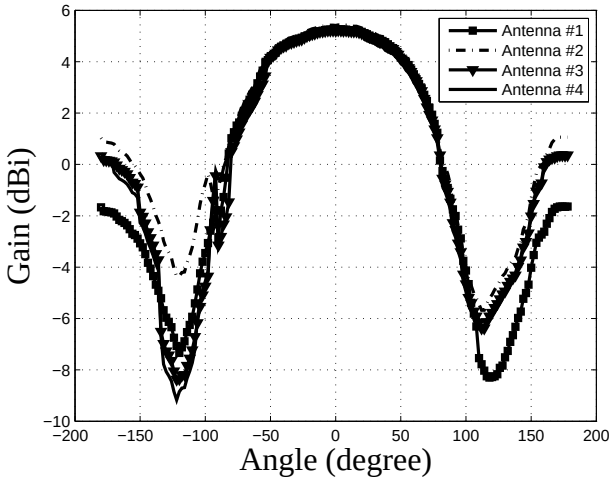


Fig. 15. Measured radiation pattern of the 4 printed Yagi antennas.

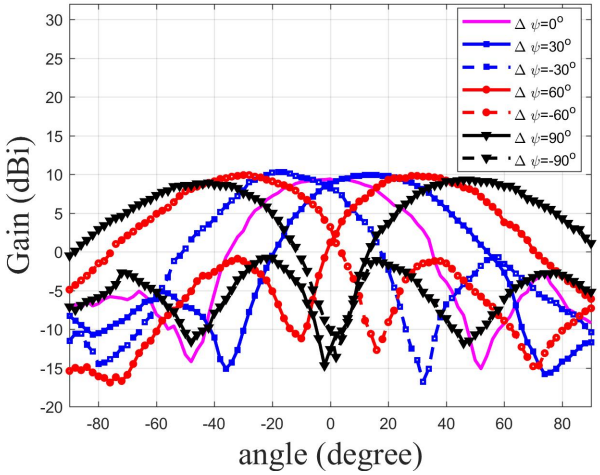


Fig. 16. Measured radiation pattern at 2.4 GHz for various $\Delta\psi$ of the uniform antenna array fed by the phase-adjustable LO signals


[3] D. Parker and D. C. Zimmermann "Phased arrayspart I: theory and architectures", *Microwave Theory and Techniques, IEEE Transactions on*, vol. 50, no. 3, pp.1039–1041, Mar 2002

[4] D. Parker and D. C. Zimmermann, "Phased arrays-part II: implementations, applications, and future trends," *Microwave Theory and Techniques, IEEE Transactions on*, vol.50, no.3, pp.688–698, Mar 2002

[5] R. C. Hansen, *Phased Array Antennas*, 2nd Edition, 2009: Wiley

[6] J. Roderick, H. Krishnaswamy, K. Newton, H. Hashemi, "Silicon-Based Ultra-Wideband Beam-Forming", *Solid-State Circuits, IEEE Journal of* , vol.41, no.8, pp.1726–1739, Aug. 2006

[7] Harry L. Van Trees, *Optimum Array Processing*, Part IV of Detection, Estimation, and Modulation Theory, 2002: Wiley

[8] Wonil Roh, Ji-Yun Seol, and et al., "Millimeter-wave beamforming as an enabling technology for 5G cellular communications: Theoretical Feasibility and prototype results", *IEEE Communications Magzine*, February, 2014.

[9] F. Ellinger, R. Vogt, W. Bachtold, "Ultracompact reflective-type phase shifter MMIC at C-band with 360 phase-control range for smart antenna combining," *Solid-State Circuits, IEEE Journal of*, vol.37, no.4, pp.481–486, Apr 2002

[10] Svetoslav Gueorguiev, Saska Lindfors, and Torben Larsen, "A 5.2 GHz CMOS I/Q Modulator With Integrated Phase Shifter for Beamforming", *Solid-State Circuits, IEEE Journal of*, vol. 42, no. 9, pp.1953–1962, September 2007

[11] Jun Yin, Wanshun Jiang, Zhigang Zhang, "A broad-band analog phase shifter design on I-Q vector modulator", *Microwave and Millimeter Wave Technology (ICMMT), 2010 International Conference on*, pp.632–635, 8-11 May 2010

[12] Ruey-Bing Hwang, Yi-Che Tsai, and et al., "A Frequency-Modulated Continuous Wave Phased Array Marine Radar System Based on Smart Antenna Technology", *Forum for Electromagnetic Research Methods and Application Technologies (FERMAT)*, vol. 5, 2014.


PLACE PHOTO HERE

**Hsien-Tung Huang** Hsien-Tung Huang received his M.S. in Institute of Communications Engineering, National Chiao Tung University (2004). He is now pursuing his PhD degree at National Chiao Tung University under the guidance of Professor Hwang. His research interest is on the phased-array radar system.

**Ruey-Bing Hwang** Ruey-Bing (Raybeam) Hwang earned his B.S. at department of Communications Engineering, National Chiao Tung University in 1990, and M.S. at department of Electrical Engineering, National Taiwan University in 1992. He received the Ph. D. degree in Institute of Electronic Engineering, National Chiao-Tung University in 1996. From August 2004 to July 2005, he was an Assistant Professor at the Communication Engineering department, National Chiao-Tung University. He became a professor of electrical engineering in August 2008. In August 2013, he was appointed Director of the Institute of Communications Engineering, which is affiliated with the ECE department. He is a honor member of Phi Tau Phi.

Professor Hwang has authored or co-authored over 30 journal publications and 50 international conference papers in the area of microwaves, optics and applied physics. Additionally, he authored a book entitled Periodic Structures: Mode-Matching Approach and Applications in Electromagnetic Engineering, published by Wiley-IEEE Press, 2013. His research interests include phased-array radar system, electromagnetic periodic structure theory, photonic crystals, and high data-rate wireless communication systems.